TISSUE ENGINEERING: Part C
Volume 29, Number 11, 2023

DOI: 10.1089/ten.tec.2023.0074

termis
Tissue Engineering
& Regenerative Medicine
International Society

Transplantation of Induced Pluripotent Stem Cell-Derived Airway Epithelia with a Collagen Scaffold into the Nasal Cavity

Yuji Kitada, MD,[1] Hiroe Ohnishi, PhD,[1] Norio Yamamoto, MD, PhD,[1,2] Fumihiko Kuwata, MD, PhD,[1] Masayuki Kitano, MD,[1] Keisuke Mizuno, MD,[1] and Koichi Omori, MD, PhD[1]

The nasal cavity is covered with respiratory epithelia, including ciliated cells that eliminate foreign substances trapped in the mucus. In hereditary diseases such as primary ciliary dyskinesia and cystic fibrosis, respiratory epithelial functions are irreversibly impaired; however, no radical treatment has been established yet. Thus, we considered that the transplantation of normal airway epithelia (AE) into the nasal epithelia is one of the strategies that could lead to radical treatment in the future. In our previous study, human induced pluripotent stem cell-derived AE (hiPSC-AE) on the vitrigel membrane were transplanted into the scraped area of the nasal septal mucosa of nude rats. Although human-derived ciliated cells, club cells, and basal cells were observed, they were located in the cysts within the submucosal granulation tissue but not in the nasal mucosal epithelia and the transplanted cells may not contribute to the function of the nasal mucosa with this condition. Therefore, to achieve more functional transplantation, we prepared the graft differently in this study by wrapping the collagen sponge in hiPSC-AE on the vitrigel membrane. As a result, we found the transplanted cells surviving in the nasal mucosal epithelia. These results suggest that hiPSC-AE transplanted into the nasal cavity could be viable in the nasal mucosa. In addition, our method leads to the establishment of nasal mucosa-humanized rats that are used for the development of the drugs and therapeutic methods for hereditary diseases of nasal respiratory epithelia.

Keywords: airway epithelia, collagen scaffold, human induced pluripotent stem cell, transplantation

Impact Statement

In hereditary diseases such as primary ciliary dyskinesia, nasal mucosal epithelia are abnormally functioning; therefore, replacing aberrant cells with normal cells by cell transplantation is a promising candidate for radical treatment. In this study, we modified the graft preparation method and achieved the survival of transplanted human-derived airway epithelia in the nasal mucosal epithelia of nude rats. These successfully transplanted cells can contribute to the functional recovery of the nasal mucosa. Our transplantation method will contribute to developing therapeutic strategies for severe nasal mucosa dysfunction caused by hereditary diseases in the future.

[1]Department of Otolaryngology-Head and Neck Surgery, Graduate School of medicine, Kyoto University, Kyoto, Japan.
[2]Department of Otolaryngology, Kobe City Medical Center General Hospital, Kobe City, Japan.

Introduction

The respiratory epithelial area, covered with the airway epithelia (AE) on the nasal mucosa, eliminates foreign substances in the inhaled air through the ciliary motility of the ciliated cells and the mucus secreted by the goblet cells.[1] The nasal mucosa has a highly regenerative capacity, and spontaneous recovery is expected even after extensive dissection by wounding or surgical excision.[2] However, in hereditary diseases such as primary ciliary dyskinesia (PCD) and cystic fibrosis (CF), airway cells are functioning abnormally, and they cannot perform their original function of eliminating foreign substances, increasing the susceptibility to infection.[3,4]

PCD, a ciliary motility disorder, is caused by $\sim$50 genetic abnormalities related to motile cilia.[5] Symptoms include refractory sinusitis, bronchiectasis, visceral retroversion, and infertility.[5] Sinusitis is mainly caused by large amounts of mucopurulent rhinorrhea rather than by polyps,[6] which always drip as posterior rhinorrhea, worsening lower respiratory tract lesions and impairing the quality of life.[7]

CF is an autosomal recessive genetic disorder caused by CF transmembrane conductance regulator gene mutations.[4] Almost all patients with CF develop chronic sinusitis. They will have characteristic viscous mucus, decreased mucociliary clearance, and chronic inflammation of the sinuses.[4] Symptoms most commonly associated with CF sinusitis include lethargy, headache, facial pain, nasal obstruction, chronic nasal congestion, and nasal discharge.[4]

CF sinusitis in children can seriously affect their quality of life because of nasal obstruction, obstructive sleep apnea, and developmental delay.[8] Sinus conditions must be improved to ameliorate adverse effects on the lower respiratory tract and improve the quality of life in patients. For pulmonary lesions, dornase alfa, hypertonic saline, and tobramycin inhalation are used to hydrolyze neutrophil-derived DNA, which is the cause of the viscous mucus and secretions in patients with CF.[9]

No radical treatment has been clinically established for irreversible dysfunction of the nasal mucosal epithelia caused by hereditary diseases such as PCD and CF. For the radical treatment of PCD and CF, several studies have been reported to regenerate function. Gene transfer studies by lentiviral vector on human primary cultured cells or transgenic mice were reported as PCD gene therapy approaches.[10,11] Genome editing using transcription activator-like effector nucleases technology has also been applied in a human primary cultured cell.[12]

Gene therapy using viral vectors has also been applied in multiple clinical trials targeting CF. In particular, gene therapy using adeno-associated viral vectors showed a good safety profile but with low efficacy in protein expression.[13] Therefore, gene therapy is one of the promising alternative treatments for these respiratory diseases. However, further research is needed to ensure treatment safety and efficacy.

Our group transplanted human induced pluripotent stem cell (hiPSC)-derived AE (hiPSC-AE) into several tissues in immunodeficient rats for the preliminary study of cell transplantation therapy and establishment of a humanized animal model. Collagen sponges wrapped in hiPSC-AE on collagen vitrigel membrane (hiPSC-AE sheet) were transplanted into nude rat tracheae.[14]

The surviving hiPSC-AE were observed at the luminal surface on the area of tracheal defects 1 and 2 weeks after transplantation.[14] The hiPSC-AE sheets were also transplanted into the mucosal defect in the middle ears of X-SCID rats.[15] Surviving cells were observed at the luminal surface of the middle ear cavity in the 1- and 2-week postoperative groups, similar to transplantation studies of tracheal defects.

In a previous study, hiPSC-AE were transplanted into the nasal mucosal epithelia of nude rats. The bone of the nasal canopy was shaved open, and hiPSC-AE on the porcine atelocollagen vitrigel membrane were applied to the scraped area of the nasal septal mucosa.[16] Although human-derived ciliated cells, club cells, and basal cells were observed 1 week after transplantation, those transplanted cells were located in the cysts within the submucosal granulation tissue but not in the nasal mucosal epithelia, Considering that the transplanted cells did not face the airway, the transplanted cells may not contribute to the function of the nasal mucosa.

Therefore, in this study, to achieve the hiPSC-AE survival within the nasal mucosal epithelium, we examined the modified transplantation method using collagen sponges as in transplantation into trachea.[14] We envision this as a future model for validation of treatments for diseases that cause intractable sinusitis.

Materials and Methods

Maintenance of hiPSC and induction of hiPSC-AE

The hiPSC line 253G1 used in this study was obtained from RIKEN BRC.[17] hiPSC maintenance and AE induction were performed in accordance with previous studies[18,19] and briefly described as follows (Fig. 1A).

The cells were maintained on Geltrex (Thermo Fisher Scientific, Waltham, MA)-coated dishes in Essential 8 Medium (Thermo Fisher Scientific) up to 10 passages. For AE induction, the hiPSCs were seeded on Geltrex-coated six-well plates in basal medium A (RPMI1640 medium [Nacalai Tesque, Kyoto, Japan] with 1×B27 supplement [Thermo Fisher Scientific] and 50 U/mL penicillin/50 mg/mL streptomycin [Thermo Fisher Scientific]) supplemented with 100 ng/mL human activin A (R&D System, Minneapolis, MN), 1 μM CHIR99021 (Axon Medchem, Groningen, Netherlands), and 10 μM Y-27632 (FUJIFILM Wako Pure Chemical Corporation, Osaka, Japan). On the next day, 0.25 mM sodium butyrate (FUJIFILM Wako Pure Chemical Corporation) was added.

From days 2 to 6, cells were treated in basal medium A supplemented with 100 ng/mL human activin A, 1 μM CHIR99021, and 0.125 mM sodium butyrate. From days 6 to 10, cells were cultured in basal medium B (DMEM/F-12 with GlutaMAX [Thermo Fisher Scientific], 1×B27 supplement, 50 U/mL penicillin/50 mg/mL streptomycin, 0.05 mg/mL L-ascorbic acid [FUJIFILM Wako Pure Chemical Corporation], and 0.4 mM monothioglycerol [FUJIFILM Wako Pure Chemical Corporation]) supplemented with 100 ng/mL human recombinant noggin (Human Zyme, Chicago, IL) and 10 μM SB431542 (Selleck Chemicals, Houston, TX).

From days 10 to 14, the cells were cultured in basal medium B supplemented with 20 ng/mL human recombinant BMP4 (Human Zyme), 2.5 μM CHIR99201, and 0.5 μM

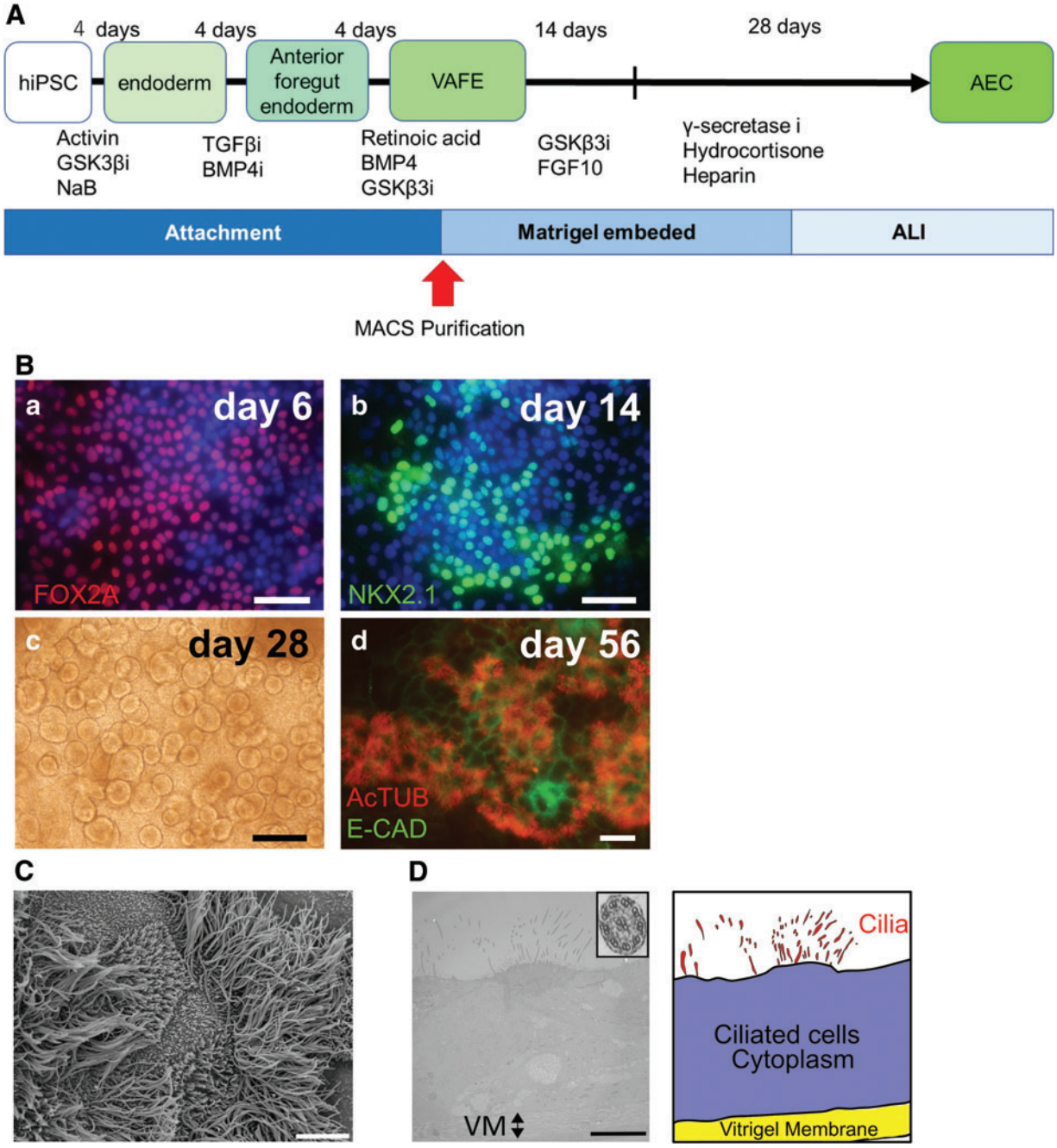

FIG. 1. Induction of hiPSC-AE. **(A)** The scheme of induction method for hiPSC-AE. VAFE, ventralized anterior foregut endoderm; AEC, airway epithelial cells; GSK3βi, CHIR99021; NaB, sodium butyrate; TGFβi, SB431542; BMP4i, noggin; γ-secretase i, DAPT; ALI, air–liquid interface culture; MACS, magnetically activated cell sorting. **(B)** Induced cells at each step in AE induction. Induced cells expressed the endoderm marker FOXA2 on day 6 (a) and the VAFE marker NKX2.1 on day 14 (b). Phase-contrast image of spheroids in Matrigel on day 28 (c). An apical surface image of the cell sheet on day 56. Airway epithelial markers, Acetylated α-tubulin (AcTUB; *red*) and E-Cadherin (E-Cad; *green*)-positive cells were observed (d). Scale bars: 50 μm (a, b), 200 μm (c), and 20 μm (d). **(C)** A scanning electron microscope image of cilia-like protrusions on the apical surface of the cell sheet on day 56. Scale bar: 5 μm. **(D)** A transmission electron microscope image (*left*) of a vertical section of cell sheet on VM on day 56 and its illustrated scheme (*right*). The *inset* shows the "9 + 2" structure, which is the specific structure of motility cilia, in cilia-like protrusions. Scale bar: 10 μm. hiPSC-AE, human induced pluripotent stem cell-derived airway epithelia; VM, vitrigel membrane. Color images are available online.

all-trans retinoic acid (Sigma-Aldrich, St. Louis, MO). On day 14, magnetically activated cell sorting method using an anti-human carboxypeptidase M (CPM) antibody (FUJIFILM Wako Pure Chemical Corporation) was performed. CPM-positive cells were embedded in a mixture of 1:1 growth factor-reduced Matrigel (Corning, NY) and basal medium B supplemented with 3.0 μM CHIR99021, 100 ng/mL FGF10 (FUJIFILM Wako Pure Chemical Corporation), and 10 μM Y-27632 on 12-well cell culture inserts with a polyethylene terephthalate membrane (No. 353292; Corning).

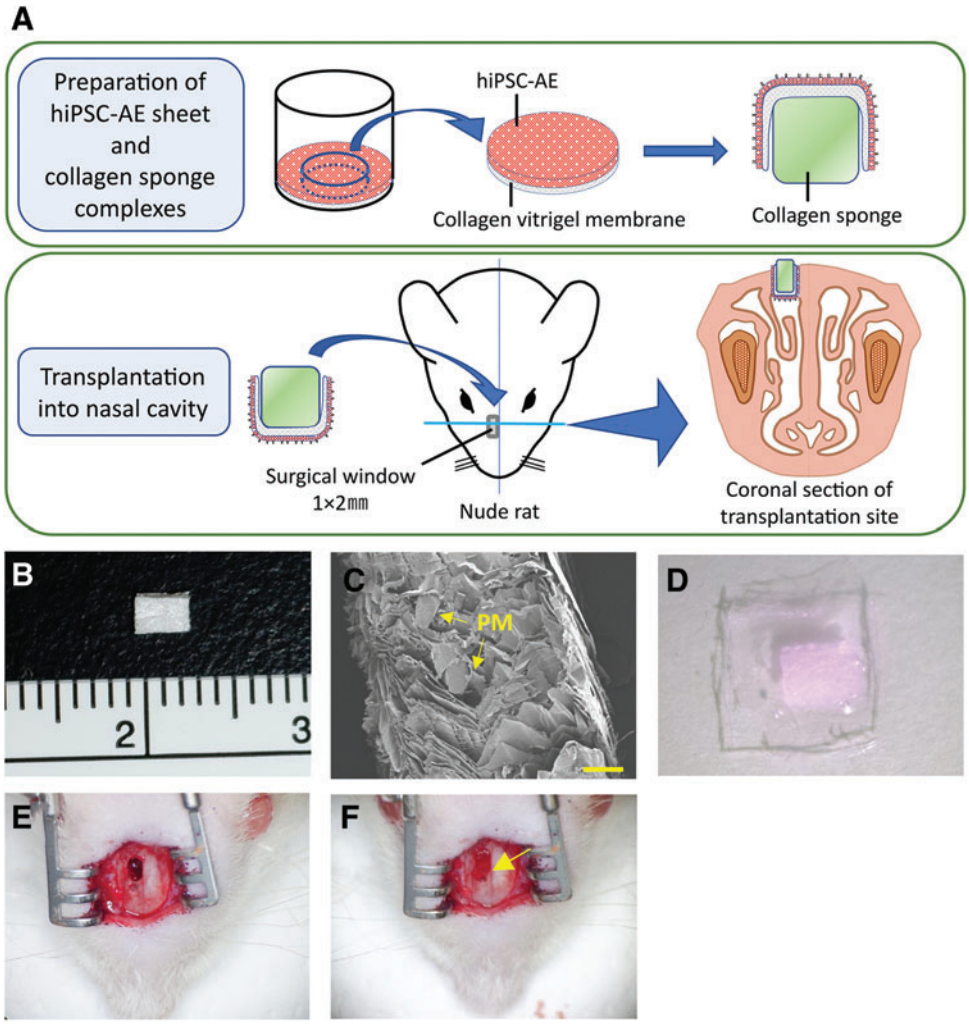

FIG. 2. Transplantation of hiPSC-AE into the nasal cavity of nude rats. **(A)** Scheme of the experimental design. For graft preparation, a small piece of collagen sponge was wrapped with a hiPSC-AE sheet. To create the defect, the right side of the internasal suture was drilled. The collagen sponge wrapped in a hiPSC-AE sheet was inserted upside down into the window so that the cell sheet was exposed to the nasal cavity. The operative site was sectioned in the direction of the *blue line*, and coronal sections were evaluated by immunohistochemistry. **(B)** A collagen sponge used as a scaffold. **(C)** Scanning electron microscope image of the vertical section of the collagen sponge. *Yellow arrows* show the stump of polypropylene mesh (PM). Scale bar: 300 μm. **(D)** Collagen sponge wrapped in a hiPSC-AE sheet. **(E)** Surgical view of a nasal cavity of a nude rat. **(F)** Surgical view of the nasal cavity of a nude rat with a graft. A *yellow arrow* indicates the graft-inserted defect. PM, polypropylene mesh. Color images are available online.

For 14 days, cells were maintained in basal medium B containing 3.0 μM CHIR99021, 100 ng/mL FGF10, and 10 μM Y-27632. From days 28 to 42, the maintenance medium was switched to PneumaCult-ALI Maintenance medium (STEMCELL Technologies, Vancouver, Canada) supplemented with 10 μM Y-27632, 4 μg/mL heparin (Nacalai Tesque), 1 μM hydrocortisone (Sigma-Aldrich), and 10 μM DAPT (FUJIFILM Wako Pure Chemical Corporation).

On day 42, the spheroids in Matrigel were dissociated into a single-cell suspension by treatment with 0.1% trypsin/EDTA (Nacalai Tesque), seeded on 12-well cell culture inserts with a collagen vitrigel membrane (ad-MED Vitrigel 2; Kanto Chemical Co., Tokyo, Japan), and maintained under air–liquid interface culture condition for 2 weeks. After 2 weeks, the induced AE on collagen vitrigel membrane were separated from the cell culture insert for transplantation as hiPSC-AE sheets (Fig. 2A).

Immunocytochemistry

Cultured cells were fixed with 4% paraformaldehyde (PFA) for 15 min, washed with phosphate-buffered saline (PBS), permeabilized with 0.2% Triton/PBS for 5 min, and incubated with 1% bovine serum albumin (BSA)/PBS for 10 min under room temperature (RT). Then, cells were treated with primary antibodies (anti-FOXA2 [Goat, AF2400, 1:500; R&D systems], NKX2.1 [mouse, MS-699-P, 1:500; Thermo Fisher Scientific], acetylated α-tubulin [AcTUB; mouse, T7451, 1:1000; Sigma-Aldrich], and E-cadherin [rat, ECCD2, 1:1000; TAKARA, Shiga, Japan] antibodies) overnight at 4°C, washed with PBS, and treated with secondary antibodies (Alexa Flour conjugated secondary antibodies [A11057, A21202, A10037, A21208, and A31573], 1:1000; Thermo Fisher Scientific) for 1 h at RT.

Nuclei were labeled with 4′,6-diamidino-pa2-phenylindole (DAPI; Thermo Fisher Scientific). Cells were embedded in Fluoromount-G® Anti-Fade (Southern Biotechnology Associates, Inc., Birmingham, AL). Images were obtained using an Eclipse Ti-S fluorescence microscope (Nikon Corporation, Tokyo, Japan) equipped with a DP73 camera (Olympus, Tokyo, Japan) or an Olympus BX 50 fluorescence microscope with a DP74 camera (Olympus).

Preparation of collagen sponge

Powdered collagen (Nippon Meat Packers, Inc., Osaka, Japan) was dissolved in pure water to a concentration of 6 mg/mL, adjusted to pH 7, and centrifuged to recover the pellet. The pellet was frozen at −80°C and lyophilized for 10

days. Then, dried collagen was cut into small pieces, dissolved in ultrapure water to a concentration of 106.4 mg/mL while adding HCl, and adjusted to pH 3. A polypropylene mesh coated with collagen solution was placed on a mold-poured collagen solution, an equal volume of the collagen solution was poured on it, and then it was frozen at −80°C overnight. After lyophilization for 1 week, collagen including polypropylene mesh was cross-linked by heating.

Electron microscopy

Cells on the vitrigel membrane were fixed with 4% PFA and 2% glutaraldehyde/PBS overnight at 4°C, incubated in 1% osmium tetroxide (Nacalai Tesque) for 2 h, and dehydrated using ascending ethanol concentrations. Dehydrated cells were dried using the critical point drying method. For scanning electron microscopy (SEM), dehydrated cells and collagen sponges were coated with platinum palladium. For transmission electron microscopy (TEM), dehydrated cells were embedded in epoxyresin and DMP-30 (Nacalai Tesque) and then sectioned. The specimens were observed under a scanning electron microscope (S-4700; Hitachi Co., Tokyo, Japan) or a transmission electron microscope (H7650; Hitachi).

Animals

Male nude rats (F344/NJcl-rnu/rnu; CLEA Japan, Osaka, Japan) aged 4–8 weeks (193–324 g) were used for transplantation experiments. The animal experimental protocol was approved by the Animal Research Committee of the Graduate School of Medicine, Kyoto University (Med Kyo 22619).

Transplantation

A total of eight male nude rats were used in the transplantation experiment under anesthesia with an intraperitoneal injection of a mixture of midazolam (2 mg/kg), butorphanol (2.5 mg/kg), and medetomidine (0.15 mg/kg). A midline skin incision was made along the internasal suture of the nasal bone. The nasal bone was exposed, and the right side of the internasal suture was drilled to open the defect in the nasal cavity. The defect size was 2 mm long and 1 mm wide.

A small piece of collagen sponge was covered with a hiPSC-AE sheet with its basal side attached to the sponge. The collagen sponge wrapped with a hiPSC-AE sheet was inserted into the nasal cavity defect with an apical side of the sheet toward the nasal cavity, and the incised skin was then sutured (Fig. 2A). One week after transplantation, rat heads were harvested, and the skin, cerebrum, eyeballs, and mandible were removed for histological examinations.

Immunohistochemistry

After overnight fixation by 4% PFA, tissues were decalcified by immersing them in 10% EDTA for 10 days and then in 10%, 20%, and 30% sucrose for 1 day each. The tissues were then embedded in Tissue-Tec optimal cutting temperature compound (Sakura Finetek Japan Co. Ltd., Tokyo, Japan). The tissues were sliced in the coronal section at a thickness of 10 μm using a cryostat (CryoStar NX70; Thermo Fisher Scientific).

All specimens were permeabilized with 0.2% Triton X-100/PBS for 5 min, washed with PBS, incubated with 5% BSA/PBS for 10 min, and treated with primary antibodies (anti-human nuclei antigen [HNA] [mouse, MAB1281, 1:1000; Millipore Darmstadt, Germany], AcTUB [mouse, T7451, 1:1000; Sigma-Aldrich], keratin 5 [rabbit, 905504, 1:500; BioLegend, San Diego, CA] and SOX2 [Goat, AF2018, 1:300; R&D Systems] antibodies).

After washing with PBS, specimens were treated with secondary antibodies (Alexa Flour conjugated secondary antibodies [A21121, A21124, A21144, A31571, A21206, A10042, A21208, and A11057], 1:1000; Thermo Fisher Scientific), phalloidin (Phalloidin CruzFluor 647, sc-363797, 1:500; Santa Cruz Biotechnology, Dallas, TX), and DAPI for 1 h at RT. After washing with PBS again, the coverslip was mounted using Fluoromount-G Anti-Fade.

Images were obtained using BZ810 (KEYENCE, Osaka, Japan). HNA and DAPI double-positive cells were defined as hiPSC-derived cells. The proportion of hiPSC-derived cells among whole epithelial cells was calculated by dividing the number of hiPSC-derived cells by that of whole DAPI-positive cells within a 200 μm width of area at the center of the nasal epithelial defect.

Results

Characterization of the cells at each induction step from undifferentiated hiPSCs to AE

In a previous study, AE were induced from 253G1 line hiPSCs on porcine atelocollagen vitrigel membrane.[16] In this study, we induced AE from 253G1 line hiPSCs on commercially available bovine collagen vitrigel, which is thinner than that used in our previous study, to replicate the tracheal transplantation study.[14] Expression of markers at each induction step was confirmed by immunocytochemical analysis (Fig. 1B). In AE induction from hiPSC, induced cells expressed endodermal cell marker FOX2A on day 6 (Fig. 1Ba), and ventralized anterior foregut endodermal cell marker NKX2.1 on day 14 (Fig. 1Bb).

On day 28, a spheroid formation was observed in Matrigel (Fig. 1Bc). After induction (day 56), cells with AcTUB-positive cilia-like structures were observed in a part of the E-cadherin-positive epithelial cell sheets (Fig. 1Bd). Moreover, these cells were examined by SEM (Fig. 1C) and TEM (Fig. 1D), and cilia-like protrusions were observed on their apical surface.

TEM images revealed the existence of ''9 + 2'' structures, consisting of nine doublet microtubules arranged in a circle around one central doublet microtubule with dynein arms, specific to motility cilia in cilia-like protrusions (Fig. 1D, inset). All morphological assessment of the cell sheet showed that the characteristics of the sheet were similar to that used in our previous study despite using thinner collagen vitrigel membrane.

Transplantation of hiPSC-AE and confirmation of transplanted cell survival in the nasal mucosal epithelia of nude rats

As another modifying point in this study, we used collagen sponges to stabilize the grafting cell sheet. The collagen sponges wrapped in the hiPSC-AE sheet were transplanted into eight nude rats (Fig. 2A). Before transplantation, the quality of collagen sponges (Fig. 2B) was examined by SEM observation. The collagen sponges have

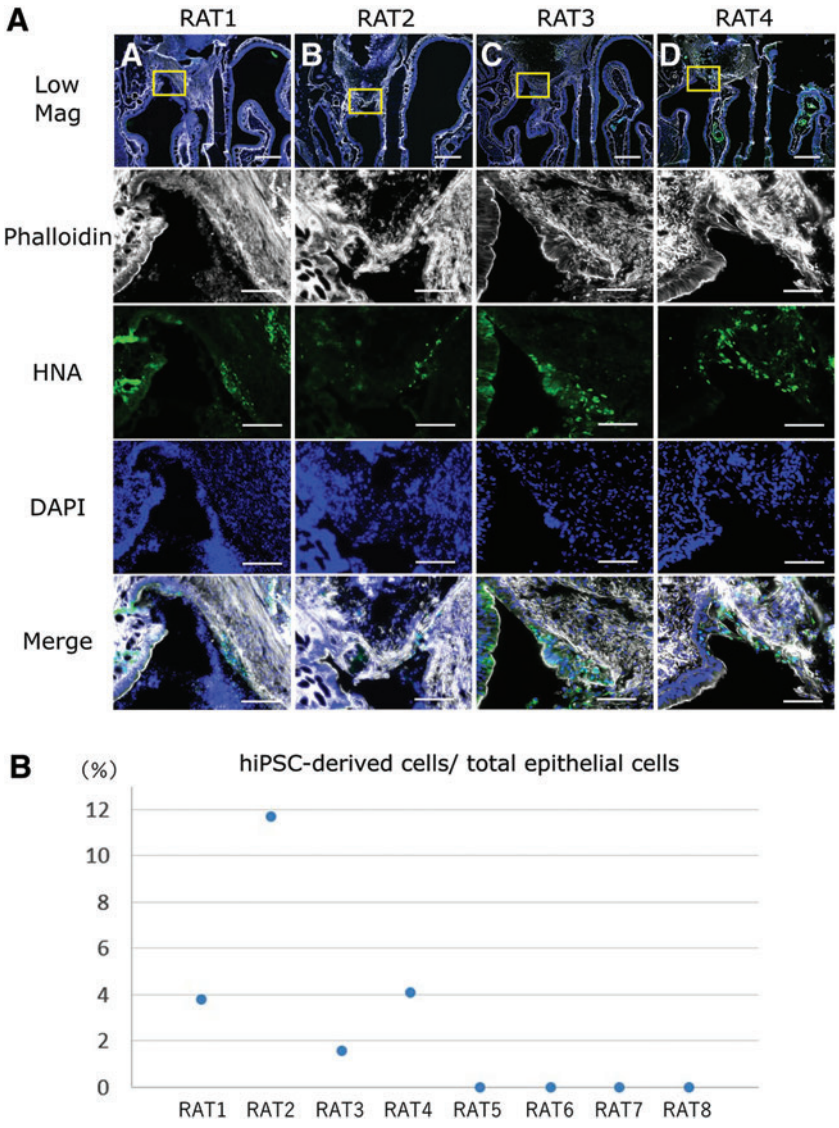

FIG. 3. Transplanted cells surviving in the nasal mucosal epithelia of nude rats. Immunohistochemical analysis revealed transplanted cells surviving in the nasal mucosal epithelia of nude rats. **(A)** Lower magnification images (LowMag) of the coronal section of the transplanted site are shown in the uppermost column. Images in the second to fifth columns are higher magnification images of the areas of the *yellow square* in the images in the uppermost column. HNA-positive cells were observed in the nasal mucosal epithelia of four nude rats. Images of DAPI staining, phalloidin staining, and their merged images are also shown. Scale bars: 500 μm for LowMag panels and 100 μm for others. The proportion of survived transplanted cells in total cells in the transplanted areas for all animals used in the experiment **(B)**. We found transplanted cells in four out of eight animals. DAPI, 4′,6-diamidino-2-phenylindole; HNA, human nuclei antigen. Color images are available online.

uniform compartments and no tears (Fig. 2C). To prepare grafts, the surface of the rectangular collagen sponge was wrapped in hiPSC-AE sheet (Fig. 2D).

The graft size was adjusted to fit into the nasal defect (Fig. 2E) and inserted upside down into the defect so that the cell sheet was exposed to the nasal cavity (Fig. 2F). One week after transplantation, the presence of hiPSC-derived cells in the epithelial layer of the nasal cavity was examined by immunohistochemical analysis. An anti-HNA antibody was used to identify hiPSC-derived cells. HNA-positive cells were identified in the nasal mucosal epithelia in four of the eight rats (Fig. 3).

In the transplanted sites, HNA-positive cells in the epithelial layer were observed in areas enclosing yellow squares in the upper column in Figure 3A. As a result of the immunohistochemical analysis of 40 sections at 50-μm intervals of specimens from each rat, HNA-positive cells in the nasal mucosal epithelia were observed in four of the eight (50%) nude rats (Fig. 3B). The proportion of survived hiPSC-derived cells in total epithelial cells within the transplanted areas were 3.8%, 11.7%, 1.6%, 4.1%, respectively (Fig. 3B).

Characterization of surviving transplanted cells in the nasal mucosal epithelia of nude rats

We examined the characterization of cell type of surviving cells in the nasal mucosal epithelia by immunohitstochemical analysis (Fig. 4). HNA-positive cells were also observed in the submucosa; however, the analyses focused only on the epithelia, which take on the role of mucociliary clearance. Some of the HNA-positive cells (Fig. 4I, J) were also positive for AcTUB, indicating that they are ciliated cells (Fig. 4E, F). Some of the HNA-positive cells (Fig. 4K, L) expressed basal cell markers SOX2 (Fig. 4G) or CK5 (Fig. 4H), indicating that they are basal cells. We examined the expressions of goblet cell marker MAC5AC and the club cell marker SCGB1A1, as well, but could not detect them in transplanted cells.

Discussion

Therapeutic methods using iPSC-derived cells are being developed for several genetic diseases, such as Duchenne muscular dystrophy and Gaucher disease.[20,21] *In vitro* disease models have also been generated using iPSCs derived

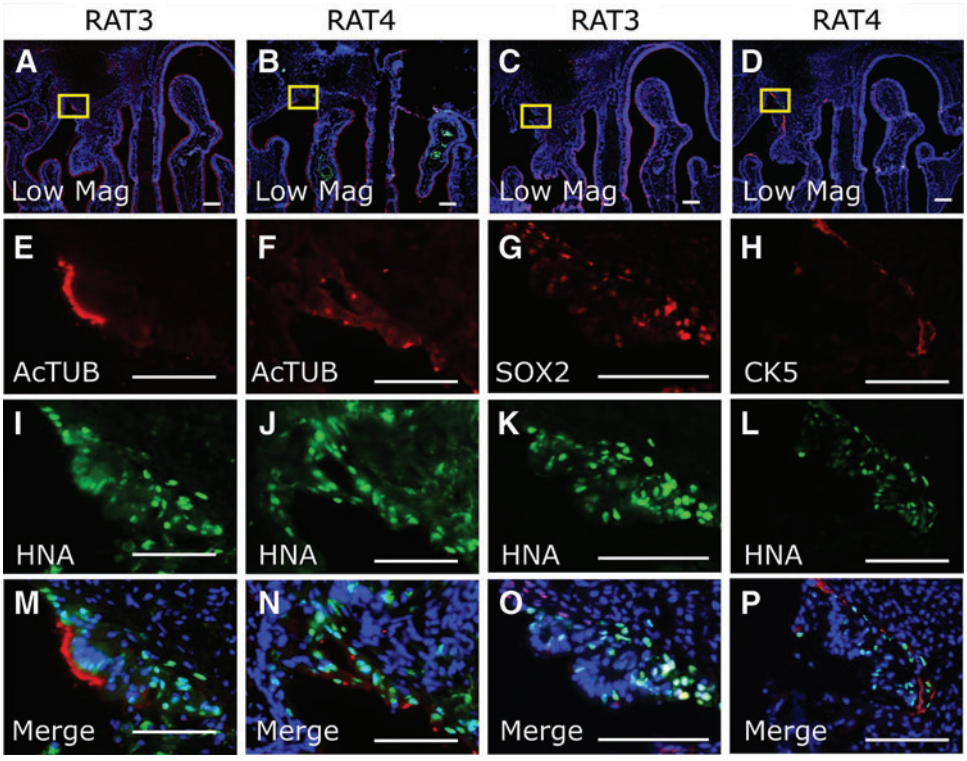

FIG. 4. Characterization of surviving cells derived from hiPSCs in the nasal mucosal epithelia of nude rats. Immunohistochemical analysis revealed the cell type of transplanted cells surviving in nude rats. Lower magnification images (LowMag) of the coronal section of the transplanted site are shown in the uppermost column **(A–D)**. **(E–P)** Higher magnification images of the areas of the *yellow square* in **A–D**. A part of surviving hiPSC-derived cells, indicated by HNA immunostaining **(I–L)**, expressing a ciliated cell marker, Acetylated α-tubulin (AcTUB; *red* **E, F**), or basal cell markers, SOX2 (*red*, **G**) or CK5 (*red*, **H**), in the nasal mucosal epithelia. Staining of nuclei by DAPI (*blue*). Scale bars: 500 μm **(A–D)**, 100 μm **(E–P)**. Color images are available online.

from patients with PCD and CF, and gene repair by genome editing has been reported.[22,23] In this study, we transplanted collagen sponges wrapped in hiPSC-AE sheets into nasal defects, and transplanted cells successfully survived in the nasal mucosal epithelia. This hiPSC-AE transplantation method may help create animal models, which make it possible to investigate functional recovery by transplantation of gene-edited cells and medicines in the future.

In this study, problems encountered in the previous study were examined, and the transplantation method was modified. In a previous study, cell sheets on thick vitrigel membranes were transplanted by pasting them onto the scraped area of the nasal septal mucosa without stabilizing the sheet.[16] As a result, HNA-positive epithelial cells were not found in the nasal mucosal epithelia but only in cysts in the submucosal tissue.

The potential reason is the constant exposure of the nasal epithelium to airflow stimulation by breathing. The airflow through the nasal cavity can cause cell sheet peel-off and make stable engraftment difficult. In addition, vitrigel membranes with a thickness of >100 μm were used in the previous study. A gap developed between the surrounding thin nasal mucosal epithelium and the transplanted cell sheets, which may have compromised the continuity with the surrounding epithelial layer.[16]

Therefore, in this study, cell sheets were prepared using a thin vitrigel membrane (<10 μm thick), and the cell sheets were placed in between the collagen sponge and the tissue in a more stable way (Fig. 2). This would fix the cell sheets in place and minimize the risk of the cell sheets shifting due to airflow. In addition, the cell sheets and nasal mucosal epithelium are always in contact with each other at both ends, which allows continuity with the neighboring mucosal epithelial layer without gaps. As a result, human-derived cells were successfully engrafted in the nasal mucosal epithelia.

In this study, the efficiency of engraftment was not high enough to be used in future studies of engrafted cell function. However, many survived transplanted cells were observed at the edge of the transplanted area, where they were in contact with recipient tissues. A possible reason is that the transplanted cells may have survived in the dented area between the graft and recipient tissue with the weakest airflow stimulation. Moreover, the possibility that the area in contact with the nasal tissue may have been supplied with factors necessary for cell survival should be considered.

In a study of cartilage regeneration by hiPSC–mesenchymal stem cell transplantation, transplanted cell-derived chondrocytes were observed in areas in contact with the recipient's cartilage.[24] Studies of hiPSC–neuronal cell transplantation have reported the improvement of the survival rate of hiPSC-derived transplanted cells by intraperitoneal administration of valproic acid and zonisamide.[25] In airway regeneration, it may be necessary to search for such factors and release them from a scaffold such as collagen at the transplant site.

Immunosuppression of the recipient animal may be essential to improve the efficiency of transplant cell engraftment. In the study of hiPSC-AE sheets transplanted into the middle ear, no transplanted cell engraftment was observed in the luminal surface mucosa in nude rats with functional defects in T cells only. In contrast, transplanted cell engraftment was observed in the luminal surface mucosa of X-SCID rats with functional defects in T, B, and NK cells.[15]

And in transplantation into the nasal cavity, the use of severe combined immunodeficiency rats with mutations in *Il2rg* and/or *Rag2* (*Il2rg* knockout, *Rag2* knockout, or *Il2rg*/

Rag2-double knockout rats)[26] may improve the efficiency of engraftment. Long-term survival was not examined in this study due to low survival efficiency of transplanted cells and should be examined in the future. Severely immunosuppressed recipients may be useful for this examination.

This study did not examine tumorigenesis, despite its importance in transplantation therapy. As only target cells were purified using CPM antibodies during AE induction,[19] contamination of undifferentiated iPSCs was deemed prevented. However, some cells may differentiate into untargeted cells during induction; indeed, human-derived mesenchymal cells have proliferated after transplantation.

Further improvements are needed, such as in purifying only epithelial cells by surface markers EpCAM[27] before seeding on the vitrigel membrane, to more strictly exclude dispensable cells. This may prevent tumorigenesis and suppress granulation at the transplant site. Long-term follow-up studies after transplantation should be performed.

After transplantation, some surviving cells were found to be positive for several airway cell markers.[28] The presence of the ciliated cell marker AcTub and HNA double-positive cells was confirmed, suggesting that this transplantation model can be used to establish a therapeutic model for hereditary diseases with abnormal cilial function, such as PCD. However, AE sheet induced with the current method did not generate ciliated cells with synchronized ciliary motility.[19]

Therefore, the application of the new method[22] to induce ciliated cells with synchronized ciliary motility should be necessary for the next step. Unlike in a previous study,[16] no club cell marker SCGB1A1 and HNA double-positive cells were identified after transplantation in this study. And no HNA-positive goblet cells were identified in the previous and current studies. However, since basal cell marker-positive cells have been identified, differentiated cells will develop from these basal cells in a similar pattern as in biological tissues. Thus, other types of AE cells must be confirmed by long-term observation in the future.

The proportion of each cell type in the hiPSC-AE sheets was also important for using as therapeutic models. The induction methods must be studied to adjust the cells in hiPSC-AE to the preferred ratio of each cell type for each disease with reference to existing induction methods.[29] The AE used in this study were prepared with the induction protocol of tracheal AE.[19] In recent years, it has been suggested from single-cell comprehensive gene expression analysis that the trachea and nasal cavity gene expression profiles are different.[30,31] Therefore, for more functional transplantation, it may be necessary to define an induction protocol optimized for the nasal cavity based on these data.

If the survival rate of transplanted cells and the cell types in surviving transplanted cells are increased by improving the induction and transplantation methods, this transplantation model can be applied not only to transplantation therapy and drug discovery but also to the study of human-specific infectious diseases such as a nasal mucosa humanized model. The limitation of this study is that we had only 1 week of observation after transplantation and did not observe the morphology of transplanted cells with electron microscopy. In the future, after the survival rate of transplanted cells improves, we will perform a long-term follow-up study by observing samples with electron microscopy 2 weeks or 3 months after transplantation.

In conclusion, hiPSC-AE were induced on commercially available thin bovine collagen vitrigel in this study. Then, the hiPSC-AE sheet was placed on the collagen sponge and transplanted into the nasal defect of nude rats. The results of the immunohistochemical analysis revealed that hiPSC-AE survived in the nasal mucosal epithelia and differentiated into the types of cells that constitute the AE, such as ciliated cells and basal cells. Thus, these results indicate that the new transplantation method established in this study may contribute to the generation of disease models and the development of cell transplantation methods.

Acknowledgments

We thank Keiko Okamoto-Furuta and Haruyasu Kohda from the Division of Electron Microscopic Study, Center for Anatomical Studies, Graduate School of Medicine, Kyoto University, for their technical support in electron microscopy and immunofluorescent microscopy using Keyence All-in-One Fluorescence Microscope BZ-X810, which were performed at the Medical Research Support Center, Graduate School of Medicine, Kyoto University, which was supported by Platform for Drug Discovery, Informatics, and Structural Life Science from the Ministry of Education, Culture, Sports, Science, and Technology, Japan.

Authors' Contributions

N.Y., H.O., and K.O. designed the study. F.K. provided critical advice for transplantation. H.O. and Y.K. prepared hiPSC-derived AEs and collagen sponge. Y.K. performed the transplantation. Y.K., F.K., M.K., K.M., and H.O. performed the histological analyses. Y.K., H.O., and N.Y. wrote the main article text and all figures. All authors participated in revising the article.

Disclosure Statement

No competing financial interests exist.

Funding Information

This study was supported by the Japan Society for the Promotion of Science (JSPS) KAKENHI (20K18279), Alumni Otolaryngology Fund from the Department of Otolaryngology-Head and Neck Surgery, Graduate School of Medicine, Kyoto University, and a joint research fund from Environmental Health Science Laboratory, Sumitomo Chemical Co., Ltd.

References

1. Bitter C, Suter-Zimmermann K, Surber C. Nasal drug delivery in humans. Curr Probl Dermatol 2011;40:20–35; doi: 10.1159/000321044
2. Ohashi Y, Nakai Y, Ikeoka H, et al. Regeneration of nasal mucosa following mechanical injury. Acta Otolaryngol Suppl 1991;486:193–201; doi: 10.3109/00016489109134996
3. Bhatt R, Hogg C. Primary ciliary dyskinesia: A major player in a bigger game. Breathe (Sheff) 2020;16(2): 200047; doi: 10.1183/20734735.0047-2020
4. Le C, McCrary HC, Chang E. Cystic fibrosis sinusitis. Adv Otorhinolaryngol 2016;79:29–37; doi: 10.1159/000444959
5. Zariwala MA, Knowles MR, Leigh MW. Primary ciliary dyskinesia. In: GeneReviews(®). (Adam MP, Everman DB,

Mirzaa GM, et al. eds.) University of Washington, Seattle Copyright © 1993–2023, University of Washington, Seattle. GeneReviews is a registered trademark of the University of Washington, Seattle. All rights reserved.: Seattle (WA); 1993.
6. Zawawi F, Shapiro AJ, Dell S, et al. Otolaryngology manifestations of primary ciliary dyskinesia: A multicenter study. Otolaryngol Head Neck Surg 2022;166(3):540–547; doi:10.1177/01945998211019320
7. Bequignon E, Dupuy L, Escabasse V, et al. Follow-up and management of chronic rhinosinusitis in adults with primary ciliary dyskinesia: Review and experience of our reference centers. J Clin Med 2019;8(9):1495; doi: 10.3390/jcm8091495
8. Ramos RT, Salles C, Gregório PB, et al. Evaluation of the upper airway in children and adolescents with cystic fibrosis and obstructive sleep apnea syndrome. Int J Pediatr Otorhinolaryngol 2009;73(12):1780–1785; doi: 10.1016/j.ijporl.2009.09.037
9. Jackson AD, Daly L, Kelleher C, et al. The application of current lifetable methods to compare cystic fibrosis median survival internationally is limited. J Cyst Fibros 2011;10(1):62–65; doi: 10.1016/j.jcf.2010.08.021
10. Chhin B, Negre D, Merrot O, et al. Ciliary beating recovery in deficient human airway epithelial cells after lentivirus ex vivo gene therapy. PLOS Genet 2009;5(3):e1000422; doi: 10.1371/journal.pgen.1000422
11. Ostrowski LE, Yin W, Patel M, et al. Restoring ciliary function to differentiated primary ciliary dyskinesia cells with a lentiviral vector. Gene Ther 2014;21(3):253–261; doi: 10.1038/gt.2013.79
12. Lai M, Pifferi M, Bush A, et al. Gene editing of DNAH11 restores normal cilia motility in primary ciliary dyskinesia. J Med Genet 2016;53(4):242–249; doi: 10.1136/jmedgenet-2015-103539
13. Bañuls L, Pellicer D, Castillo S, et al. Gene therapy in rare respiratory diseases: What have we learned so far? J Clin Med 2020;9(8); doi: 10.3390/jcm9082577
14. Okuyama H, Ohnishi H, Nakamura R, et al. Transplantation of multiciliated airway cells derived from human iPS cells using an artificial tracheal patch into rat trachea. J Tissue Eng Regen Med 2019;13(6):1019–1030; doi: 10.1002/term.2849
15. Tada T, Ohnishi H, Yamamoto N, et al. Transplantation of a human induced pluripotent stem cell-derived airway epithelial cell sheet into the middle ear of rats. Regen Ther 2022;19:77–87; doi: 10.1016/j.reth.2022.01.001
16. Kuwata F, Ohnishi H, Yamamoto N, et al. Transplantation of human induced pluripotent stem cell-derived airway cells on vitrigel membrane into rat nasal cavity. Tissue Eng Part A 2022;28(13–14):586–594; doi: 10.1089/ten.TEA.2021.0071
17. Nakagawa M, Koyanagi M, Tanabe K, et al. Generation of induced pluripotent stem cells without Myc from mouse and human fibroblasts. Nat Biotechnol 2008;26(1):101–106; doi: 10.1038/nbt1374
18. Gotoh S, Ito I, Nagasaki T, et al. Generation of alveolar epithelial spheroids via isolated progenitor cells from human pluripotent stem cells. Stem Cell Rep 2014;3(3):394–403; doi: 10.1016/j.stemcr.2014.07.005
19. Konishi S, Gotoh S, Tateishi K, et al. Directed induction of functional multi-ciliated cells in proximal airway epithelial spheroids from human pluripotent tem cells. Stem Cell Rep 2016;6(1):18–25; doi: 10.1016/j.stemcr.2015.11.010
20. Miura Y, Sato M, Kuwahara T, et al. Transplantation of human iPSC-derived muscle stem cells in the diaphragm of Duchenne muscular dystrophy model mice. PLoS One 2022;17(4):e0266391; doi: 10.1371/journal.pone.0266391
21. Panicker LM, Srikanth MP, Castro-Gomes T, et al. Gaucher disease iPSC-derived osteoblasts have developmental and lysosomal defects that impair bone matrix deposition. Hum Mol Genet 2018;27(5):811–822; doi: 10.1093/hmg/ddx442
22. Sone N, Konishi S, Igura K, et al. Multicellular modeling of ciliopathy by combining iPS cells and microfluidic airway-on-a-chip technology. Sci Transl Med 2021;13(601); doi: 10.1126/scitranslmed.abb1298
23. Crane AM, Kramer P, Bui JH, et al. Targeted correction and restored function of the CFTR gene in cystic fibrosis induced pluripotent stem cells. Stem Cell Rep 2015;4(4):569–577; doi: 10.1016/j.stemcr.2015.02.005
24. Yoshimatsu M, Ohnishi H, Zhao C, et al. In vivo regeneration of rat laryngeal cartilage with mesenchymal stem cells derived from human induced pluripotent stem cells via neural crest cells. Stem Cell Res 2021;52:102233; doi: 10.1016/j.scr.2021.102233
25. Nishimura K, Takata K. Combination of drugs and cell transplantation: More beneficial stem cell-based regenerative therapies targeting neurological disorders. Int J Mol Sci 2021;22(16); doi: 10.3390/ijms22169047
26. Miyasaka Y, Wang J, Hattori K, et al. A high-quality severe combined immunodeficiency (SCID) rat bioresource. PLoS One 2022;17(8):e0272950; doi: 10.1371/journal.pone.0272950
27. Gires O, Kieu C, Fix P, et al. Tumor necrosis factor alpha negatively regulates the expression of the carcinoma-associated antigen epithelial cell adhesion molecule. Cancer 2001;92(3):620–628; doi: 10.1002/1097-0142(20010801)92:3<620::aid-cncr1362>3.0.co;2-f
28. Davis JD, Wypych TP. Cellular and functional heterogeneity of the airway epithelium. Mucosal Immunol 2021;14(5):978–990; doi: 10.1038/s41385-020-00370-7
29. Yu F, Liu F, Liang X, et al. iPSC-derived airway epithelial cells: Progress, promise, and challenges. Stem Cells 2023;41(1):1–10; doi: 10.1093/stmcls/sxac074
30. Deprez M, Zaragosi LE, Truchi M, et al. A single-cell atlas of the human healthy airways. Am J Respir Crit Care Med 2020;202(12):1636–1645; doi: 10.1164/rccm.201911-2199OC
31. Paranjapye A, Leir SH, Huang F, et al. Cell function and identity revealed by comparative scRNA-seq analysis in human nasal, bronchial and epididymis epithelia. Eur J Cell Biol 2022;101(3):151231; doi: 10.1016/j.ejcb.2022.151231

Address correspondence to:
Norio Yamamoto, MD, PhD
Department of Otolaryngology-Head and Neck Surgery
Graduate School of Medicine
Kyoto University
54 Shogoin Kawahara-cho, Sakyo-ku
Kyoto city
Kyoto 606-8507
Japan

E-mail: yamamoto@ent.kuhp.kyoto-u.ac.jp

Received: April 8, 2023
Accepted: August 22, 2023
Online Publication Date: October 19, 2023